Hindawi Publishing Corporation
Mathematical Problems in Engineering
Volume 2012, Article ID 498690, 14 pages
doi:10.1155/2012/498690

Research Article

Particle Swarm Optimization Algorithm Coupled with Finite Element Limit Equilibrium Method for Geotechnical Practices

Hongjun Li,[1] Hong Zhong,[2] Zuwen Yan,[1] and Xuedong Zhang[1]

[1] *State Key Laboratory of Simulation and Regulation of Water Cycle in River Basin, China Institute of Water Resources and Hydropower Research, Beijing 100048, China*
[2] *Faculty of Infrastructure Engineering, Dalian University of Technology, Dalian 116024, China*

Correspondence should be addressed to Hongjun Li, lijunli1995@163.com

Received 5 October 2012; Accepted 10 November 2012

Academic Editor: Fei Kang

This paper proposes a modified particle swarm optimization algorithm coupled with the finite element limit equilibrium method (FELEM) for the minimum factor of safety and the location of associated noncircular critical failure surfaces for various geotechnical practices. During the search process, the stress compatibility constraints coupled with the geometrical and kinematical compatibility constraints are firstly established based on the features of slope geometry and stress distribution to guarantee realistic slip surfaces from being unreasonable. Furthermore, in the FELEM, based on rigorous theoretical analyses and derivation, it is noted that the physical meaning of the factor of safety can be formulated on the basis of strength reserving theory rather than the overloading theory. Consequently, compared with the limit equilibrium method (LEM) and the shear strength reduction method (SSRM) through several numerical examples, the FELEM in conjunction with the improved search strategy is proved to be an effective and efficient approach to routine analysis and design in geotechnical practices with a high level of confidence.

1. Introduction

Slope stability analysis is still a hot issue and complex problem in the field of geotechnical engineering, which has been attracting the attention of many geotechnical researchers. Nowadays, the limit equilibrium method (LEM), the shear strength reduction method (SSRM), and the finite element limit equilibrium method (FELEM) are generally employed in geotechnical practices by engineers and researchers.

The LEM is a conventional and well-defined approach due to its simplicity and applicability. It can handily evaluate the stability of soil slope via the minimum factor of safety and associated critical failure surface. However, the major limitation of the LEM is

that it is established based on some assumptions on the distributions of internal forces or the normal force within the rigid slices. In addition, the LEM requires many trial failure surfaces and great effort to locate the critical failure surface. Recently, many advanced heuristic global optimization methods have been proposed successfully and detailed discussion on these methods for the special N-P type global optimization problem has been provided by Cheng et al. [1–6]. Unfortunately, for a nonhomogeneous soil slope, whose mechanical properties change with time and stress state, the LEM built on rigid plastic theory might be unreasonable.

Since the first application of the Shear strength reduction method (SSRM) in slope stability analysis by Zienkiewicz et al. [7], thorough studies on the approach have been carried out by Griffiths and Lane [8], Cheng et al. [9], and others. Assumptions on the shape and location of the critical slip surface for this technique are unnecessary. In addition, it can depict directly the process of progressive failure through display of strain field or displacement field for soil slopes. However, Cheng et al. [9] have conducted an extensive comparison between the LEM and SSRM and pointed out two major critical limitations of the SSRM, as follows: (i) it is hard to achieve a good evaluation for a soil slope with soft band; (ii) the results obtained from the SSRM are sensitive to the FEM mesh, the choice of the tolerance and the solution of the nonlinear equations, convergence criterion, constitutive model and boundary condition, and so on.

The finite element limit equilibrium method, which effectively couples the limit equilibrium method and finite element stress analysis, can quickly obtain the factor of safety under actual stress field. In the past decades, the FELEM for circular slip surface has been well established and applied successfully into the stability analysis of soil slopes due to its simplicity and practicability by Zou et al. [10], Kim and Lee [11], Pham and Fredlund [12], Yamagami and Ueta [13], and Shao et al. [14]. In addition, the simplex method, dynamic programming, and leap-frog method have been successfully introduced into the search of the critical slip surfaces. However, most of the above-mentioned studies are limited to circular slip surface. Consequently, the two issues, (i) whether the FELEM is suitable for the stability analysis with noncircular slip surface and (ii) whether the modern heuristic optimization techniques which have been employed successfully in the LEM are suitable for the FELEM to search for the critical non-circular failure surface, still puzzle the researchers and geotechnical engineers. Thus, before introducing the FELEM associated with the non-circular slip surface into routine practice and design in geotechnical engineering, the following three key problems must be figured out: (i) the definition and physical meaning of factor of safety for non-circular slip surface in the FELEM; (ii) the effective and efficient optimization algorithm to determine the global minimum factor of safety and associated critical non-circular slip surface; (iii) the relationships of the minimum factor of safety and location of critical non-circular slip surface in the LEM, SSRM, and FELEM in routine geotechnical practices.

In this paper, the factor of safety for non-circular slip surface in the FELEM is derived from the necessary and sufficient conditions making the sliding body reaches the critical limit equilibrium state. The particle swarm optimization algorithm for searching the critical non-circular slip surface which was adopted in the LEM by Cheng et al. [15] is modified to couple with the FELEM. In the modified particle swarm optimization method, the requirements of a kinematically acceptable failure mechanism and stress compatibility mechanism are presented. Finally, the factors of safety and the locations of associated critical non-circular

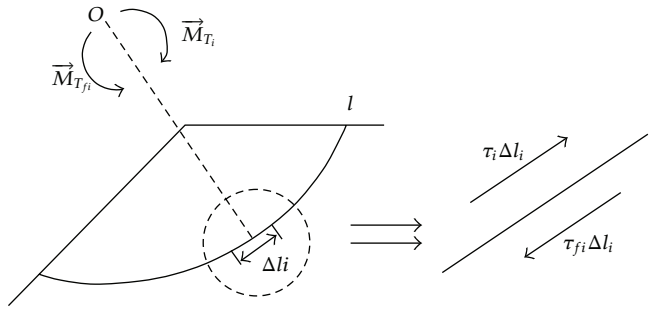

Figure 1: Equilibriums of force and moment in a segment of the slip surface.

failure surfaces obtained by the FELEM, LEM, and SSRM are compared for various soil slopes.

2. Formulation of Necessary and Sufficient Conditions

As represented in Figure 1, given l as a continuous slip surface for arbitrary shape in soil slope, the critical limit equilibrium state for the sliding body implies that the shear force and moment counterpoise the resistant shear force and moment in any segment (Δl_i) of the slip surface. Meanwhile, the integral of the sliding force and moment counterpoises that of the resistant sliding force and moment along the slip surface. The relationships of force and moment equilibrium in one segment of slip surface are depicted in Figure 1. Explicit expressions for the above-defined critical limit equilibrium state are obtained in (2.1a)~(2.3):

$$\vec{T}_i - \vec{T}_{fi} = 0, \quad i = 1, n, \tag{2.1a}$$

$$\vec{M}_{\vec{T}_i} - \vec{M}_{\vec{T}_{fi}} = 0, \quad i = 1, n. \tag{2.1b}$$

Summarizing both sides of (2.1a) and (2.1b) from 1 to n, the following relations are obtained:

$$\sum_{i=1}^{n} \vec{T}_i - \sum_{i=1}^{n} \vec{T}_{fi} = 0, \tag{2.2}$$

$$\sum_{i=1}^{n} \vec{M}_{\vec{T}_i} - \sum_{i=1}^{n} \vec{M}_{\vec{T}_{fi}} = 0, \tag{2.3}$$

where $\vec{T}_i$, $\vec{M}_{\vec{T}_i}$, $\vec{T}_{fi}$, and $\vec{M}_{\vec{T}_{fi}}$ represent the driving force and moment, resistant sliding force, and moment acted on segment i of the slip surface, respectively; τ_i and τ_{fi} are the shear stress and resistant shear strength of the segment i; Δl_i is the length of segment i; n represents the number of segments constituting the failure surface l.

It will be proved that the necessary and sufficient condition for the equilibrium between the driving force and the resistant sliding force in any segment of the slip surface

can be expressed by (2.4) as the sliding body reaches the steady state; namely, the integration of shear stress equals to that of resistant shear strength along the slip surface l:

$$\int_l \tau \, dl = \int_l \tau_f dl. \tag{2.4}$$

Firstly, given that the driving force equals to the resistant sliding force in any segment of failure surface, which validates (2.1a), then (2.2) can be achieved. The derivations are presented as follows.

The force equilibrium of segment i in the tangential direction gives

$$\tau_i \cdot \Delta\vec{l}_i - \tau_{fi} \cdot \Delta\vec{l}_i = 0. \tag{2.5}$$

Then (2.5) can be rewritten into the following form:

$$(\tau_i \cdot \Delta l_i - \tau_{fi} \cdot \Delta l_i)\vec{l}_i = 0, \tag{2.6}$$

where $\vec{l}_i$ is the direction vector of segment i in the tangential direction.

If (2.6) is justified, (2.7) can be achieved by transforming (2.6) into a scalar form:

$$\tau_i \cdot \Delta l_i - \tau_{fi} \cdot \Delta l_i = 0. \tag{2.7}$$

Then by summarizing both sides of (2.7) from 1 to n, (2.4) can be formulated in another form:

$$\sum_{i=1}^{n} \tau_i \cdot \Delta l_i - \sum_{i=1}^{n} \tau_{fi} \cdot \Delta l_i = 0. \tag{2.8}$$

Secondly, if (2.4) or (2.8) is tenable, the equation can be rewritten as

$$\sum_{i=1}^{n} (\tau_i - \tau_{fi}) \cdot \Delta l_i = 0. \tag{2.9}$$

By considering the stress compatibility mechanism for all the segments of the slip surface reaching the critical equilibrium state, the additional stress compatibility restriction of failure surface should be guaranteed as follows:

$$\tau_i \le \tau_{fi}. \tag{2.10}$$

Considering the restriction condition, if (2.9) can be satisfied, then (2.11) must be justified:

$$\tau_i \cdot \Delta l_i - \tau_{fi} \cdot \Delta l_i = 0. \tag{2.11}$$

Then, (2.1a)~(2.3) are resulted.

It is noted that for the sliding body being in a critical limit equilibrium state along the surface l, (2.1a), (2.1b) and (2.4) must be satisfied. So the necessary and sufficient conditions for the sliding body reaching the critical limit equilibrium state along the surface l can be expressed in

$$\frac{\int_l \tau_f dl}{\int_l \tau \, dl} = 1. \tag{2.12}$$

3. Factor of Safety in FELEM

Apparently, the definition of factor of safety F_s which can be provided with reasonable physical meaning is the most important issue in the slope stability analysis. So far, there are two commonly used definitions. The first is based on the strength reserving theory, which defines F_s as the coefficient by which the shear strength of the soil would be reduced to drive the slope into the critical limit equilibrium state. The second definition is based on the overloading theory, which obtains the F_s as the ratio of the ultimate limit loading that militates the occurrence of slope failure to the insitu loading acting on the soil slope. In the LEM, the strength reserving theory which is utilized to form the equilibrium equations of slices is formulated to solve the statically indeterminate problem. Likewise, in the SSRM, F_s is also derived through the strength reserving theory, which assumes that while c and φ are reduced simultaneously by an efficient, the slip failure would initially trigger in soil slope.

In the FELEM, given that F_s (l) is the function of strength reduction coefficient for segments along the surface l, that is, (2.1a) and (2.1b) can be achieved by dividing the shear strength by the function in any segment of the sliding surface l, and then the necessary and sufficient conditions for the sliding body along the surface l reaching the critical limit equilibrium state (2.12) can be rewritten as

$$\int_l \frac{\tau_f}{F_s(l)} dl = \int_l \tau \, dl. \tag{3.1}$$

Based on the mean value theorem, the left side of (3.1) can be transformed into

$$\int_l \frac{\tau_f}{F_s(l)} dl = \frac{\int_l \tau_f dl}{F_s}. \tag{3.2}$$

According to (3.1) and (3.2), the factor of safety in the FELEM can be formulated as

$$F_s = \frac{\int_l \tau_f dl}{\int_l \tau dl}. \tag{3.3}$$

Based on the above derivations, it is proved that the definition of factor of safety in the FELEM is also established on the strength reserving theory as in the LEM and SSRM. Futhermore, the physical meaning of factor of safety in the FELEM is the average strength reduction coefficient for the whole potential sliding body reaching the critical limit equilibrium state along the slip surface.

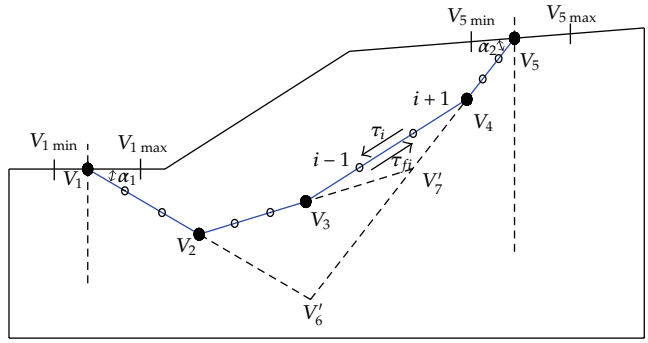

Figure 2: Generation of reasonable failure surface.

4. Modified Particle Swarm Optimization Algorithm in FELEM

In this paper, a modern search procedure based on a modified particle swarm optimization algorithm is proposed. In the modified approach, the method of generating trial failure surfaces which are kinematically acceptable and stress compatibility is similar to that by Cheng et al. [15], Greco [16], and Malkawi et al. [17].

Considering the trial surface with four segments and five vertices (V_1, V_2, V_3, V_4, and V_5) shown in Figure 2, it can be represented by eight control variables including x_1, x_5, α_1, α_2, δ_1, δ_2, δ_3, and δ_4. Here x_1 and x_5 are the horizontal coordinates of the initial point, and end point rerspectively; α_1 and α_2 are the initial angle and end angle. $\delta_1, \delta_2, \ldots, \delta_4$ are random numbers in the range $(-0.5, 0.5)$. Implementation of the trial slip surface includes the following steps: (i) the initial point and end point are determined based on the given lower bound and upper bound; (ii) the α_1 and α_2 are achieved by the random procedure in the range $(0, \pi/2)$ until the reasonable intersection points of V_{16}' and V_{56}' (Figure 2) are obtained; (iii) the positions of V_2 and V_7' are loacated according to the random numbers δ_1 and δ_2; (iv) the positions of V_3 and V_4 are achieved based on the random numbers δ_3 and δ_4 between the two adjacent segments which have the largest horizontal distance. Herein, according to the above principle, the specified number of vertices or segments can be produced. However, although the trial slip surfaces generated by the above procedure are kinematically admissible, the stress compatability condition for these trial failure surfaces cannot be guaranteed strictly, which means that (2.10) may not be satisfied. Thus, the segments constituting the slip surface should be subdivided to make sure that the stress constraint condition is met.

Based on the above descriptions, the formulations for a typical slope stability analysis can be written as follows:

$$\min \quad Fs(x), \tag{4.1}$$

$$\text{s.t.} \quad x_l \le x_1 \le x_u; \quad x_l \le x_{n+1} \le x_u, \tag{4.2}$$

$$\text{s.t.} \quad 0 < \alpha_1 < \frac{\pi}{2}; \qquad 0 < \alpha_2 < \frac{\pi}{2}, \tag{4.3}$$

$$\text{s.t.} \quad 0 < \delta_i < 0.5, \quad i = 1, 2n - 4, \tag{4.4}$$

$$\text{s.t.} \quad \tau_i \le \tau_{fi}, \quad i = 1, n \times m, \tag{4.5}$$

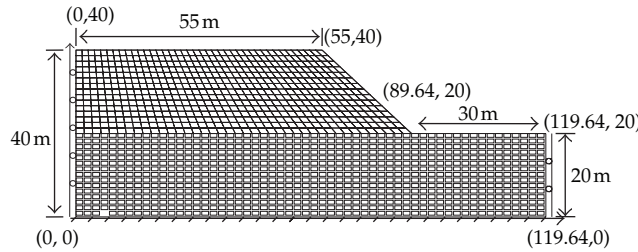

Figure 3: Mesh for a homogeneous soil slope.

where n is the number of segments constituting the slip surface; m is the number of subdivisions of one segment. In fact, the constraint condition (4.5) has little effect on the results, but it can guarantee the stress compatibility of slip surface and achievement of necessary and sufficient conditions.

Recently, the particle swarm optimization (PSO) which is a modern heuristic global optimization algorithm has been broadly used in complex continuous optimization problems [18, 19]. However, it is noted that the accuracy and efficiency for the method cannot be guaranteed as the number of control variables becomes more. To obtain the optimized solution with fewer trials, a new version called Modified PSO (MPSO) was developed by Cheng [1]. In MPSO, only several particles which have better objective function values are allowed to fly. In the flying procedures, several flies are allowed for each particle in the group; that is, one particle can fly more than once according to its objective function value. The better the objective function value of one particle, the more times it is allowed to fly. Herein, the number of speciated flies does not represent the number of speciated particles that can fly. After the specified flies are achieved, the objective function value of these flies is checked. Then new position and velocity are randomly chosen for the particles which have the chance to fly more than once for the next circle and other new positions and velocities will be assigned randomly to those nonflying particles in the current iteration. Other procedures of the applied method not mentioned here are the same as the original particle swarm optimization.

5. Verifications

Based on the above formulations and derivations, the authors have developed a program FELEM-2D and five typical examples are used for the thorough study of the FELEM in geotechnical practices. For the LEM, the Spencer method, which satisfies both moment and force equilibrium, is adopted. The critical failure surfaces in the LEM and FELEM are achieved by the combination of the modified Particle swarm optimization method (MPSO). The inertial weight coefficient is 0.5. The stochastic weighting coefficients are 2.0. The number of iterations is 200. The specified number of segments and flies in one iteration is 30 and 15, respectively. For the SSRM, the plastic strain is used to depict the critical failure surface and the failure to converge is adopted as the failure criterion for a soil slope. In addition, the elastic perfectly plastic model with nonassociated flow law and Mohr-Coulomb failure principle is incorporated into the finite element stress analysis in the FELEM and SSRM.

Example 5.1 (Homogeneous soil slope). Firstly, a homogeneous soil slope (Figure 3) [20] is adopted. The intensity properties and unit weight of the soil are 42 kPa, 17°, and 25 kN/m^3,

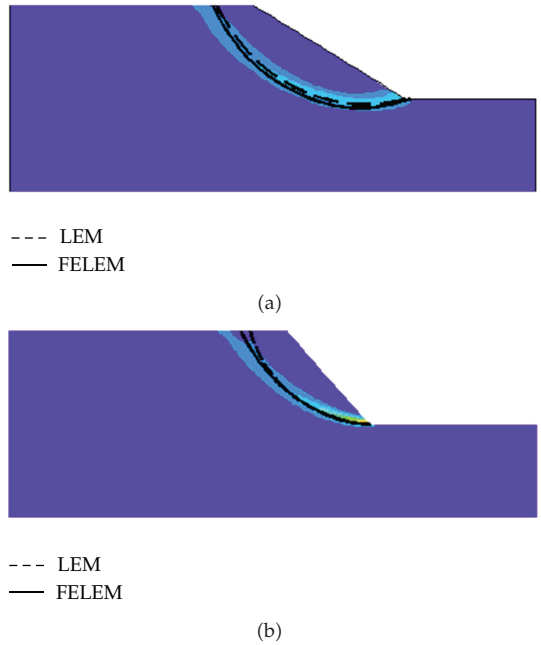

Figure 4: Comparisons of critical slip surfaces for two slope inclinations: (a) 30°; (b) 50°.

Table 1: Factors of safety by the LEM, SSRM and FELEM.

Methods	Slope inclination				
	30°	35°	40°	45°	50°
FELEM	1.408	1.287	1.178	1.075	1.007
SSRM	1.390	1.260	1.150	1.070	1.000
LEM	1.392	1.260	1.152	1.063	0.985

respectively. In the study, the slope with different slope inclinations are considered and the LEM, SSRM, and FELEM analyses are carried out. The slope inclination of 30°, 35°, 40°, 45°, and 50° are studied, respectively. The elastic modulus and Poisson's ratio of the soil are assumed to be 10 MPa and 0.3, respectively, throughout the numerical examples in this paper unless specified. The boundary conditions are depicted in Figure 3. The stress field is obtained by the well-known commercial geotechnical finite element programs Z-SOIL. The results of stability analysis from the LEM and SSRM are obtained through SLIDE5.0 and Z-SOIL, respectively.

In Figure 4, the dashed curves and the solid curves denote the critical slip surface obtained by the LEM and the FELEM, respectively, while the shade zones (plastic strain) denote the potential sliding surface obtained by the SSRM. From Table 1 and Figure 4, it is found that the factor of safety and associated critical failure surface determined by the LEM, SSRM, and FELEM are fairly consistent for different slope inclinations. Based on the same shear strength parameters, all the factors of safety obtained by the LEM and SSRM differ by less than 3% with respect to the FELEM with the increase of slope inclination. Since the results obtained by the LEM, SSRM, and FELEM are in good agreement and only minor

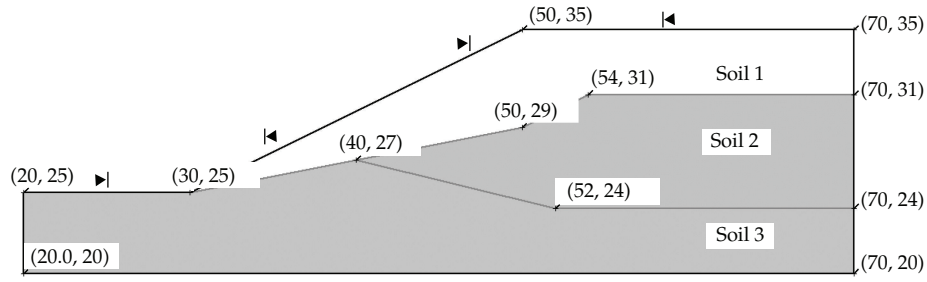

Figure 5: Geometry of a nonhomogeneous soil slope.

Table 2: Parameters of soil material.

Soil	c/kPa	$\phi/(^\circ)$	$\gamma/(\mathrm{kN/m^3})$	$E/(\mathrm{kPa})$	μ	K_0
1	0	38	19.5	10000	0.25	0.65
2	5.3	23	19.5	10000	0.25	0.65
3	7.2	20	19.5	10000	0.25	0.65

differences exist, it can be concluded that the performances of the LEM, SSRM, and FELEM are all satisfactory for the case of homogeneous soil slope.

Example 5.2 (Nonhomogeneous soil slope). In this example, the proposed method in conjunction with the MPSO is employed for analysis of a nonhomogeneous soil slope (Figure 5). Table 2 gives the geotechnical parameters for this example. The stress field is obtained by the Z-SOIL. The results of stability analysis from the LEM and SSRM are obtained through SLIDE5.0 and PLAXIS, respectively.

Figures 6 and 7 show the non-circular critical slip surfaces with 30 segments obtained by the LEM (Spencer) the SSRM and the FELEM, respectively. The factors of safety and associated critical failure surfaces are in good agreement with the LEM, SSRM, and FELEM as can be seen from Table 3 and Figures 6 and 7. It is noted that the right end of slip surface moves closer to the crest of the slope in the LEM and FELEM.

Example 5.3 (Slope with a soft band). A soil slope with a thin soft band (Figure 8) [21] which was considered by Griffiths and Lane [8] is studied. The friction angles of both the soft band and surrounding soil are equal to be zero. The unit weight, elastic modulus, and Poisson's ratio of the two soils are the same, with the value shown in Example 5.1. c_{u2} and c_{u1} are the strengths of the soft band and the surrounding soil, respectively. $c_{u1}/\gamma H = 0.25$ holds for the surrounding soil.

Considering the effect of the ratio c_{u2}/c_{u1} in the LEM, SSRM, and FELEM, the stability analysis is conducted with six strength ratios that range between 0.4 and 1.0. The results are listed in Table 4 and the associated critical sliding surfaces obtained by the SSRM and FELEM for two typical cases are depicted in Figures 9 and 10.

From Table 4 and Figures 9 and 10, it can be found that the minimum factors of safety and associated critical failure surfaces achieved by the FELEM are in good agreement with the SSRM. The locations of the critical failure surfaces from the SSRM and FELEM for the strength ratios from 0.6 to 1.0 are virtually similar. However, it is noted that the critical failure surface is obviously sensitive to the strength parameters of the soft band. The non-circular failure surfaces, as shown in Figures 9 and 10, are almost along the soft band as the strength

Table 3: Factors of safety by the LEM, SSRM, and FELEM.

Method	Factor of safety
FELEM (Mohr-Coulomb principle)	1.382
SSRM (Mohr-Coulomb principle)	1.324
Simplified Bishop	1.394
Spencer	1.373

Table 4: Factors of safety by the SSRM and FELEM.

Methods	c_{u2}/c_{u1}					
	0.4	0.5	0.6	0.7	0.8	1.0
FELEM	—	1.166	1.373	1.409	1.430	1.456
SSRM	0.990	1.215	1.370	1.400	1.420	1.455

ratio is below 0.6. As the ratio of c_{u2} and c_{u1} is above 0.6, the circular failure mechanism governs the stability of slope, and the factor of safety is essentially irrelevant of the strength of soft band. Furthermore, it is noted that the proposed method cannot achieve the factor of safety and the location of failure surface as the given strength ratio is below 0.5, because in the special case the plastic finite element stress analysis cannot obtain a convergent solution, which means that the actual stress field for the soil slope cannot be determined.

Example 5.4 (Soil slope under steady-state seepage). A homogeneous slope with free surface shown in Figure 11 has the same geotechnical parameters and FEM mesh as in Example 5.1.

Regarding the role of the seepage, the SEEP/W is conducted to achieve the distribution of pore pressure in soil slope. In the elastic-plastic FEM analysis, the effective stress of each gauss point can be used in the stability analysis by subtracting the pore pressure from the total stress. The factor of safety of the slope has been determined for several different slope inclinations, which varies from 30° to 50°. The comparisons for the minimum factor of safety are shown in Table 5.

Excellent agreements concerning the minimum factors of safety between the three methods are observed from the above results.

Example 5.5 (Ultimate bearing capacity for soil footing). Formerly, the ultimate bearing capacity of soil footing, which is usually regarded as the external loading which can drive the soil footing into onset of failure, can be obtained by the LEM, limit analysis. For the special example (Figure 12) [21], Griffiths got limit collapse loading for soil footing by elastic-plastic finite element method based on a single failure criterion of misconvergence. In the present paper, the FELEM is performed to determine the ultimate bearing capacity of soil footing, implying that an additional failure criterion that the factor of safety of critical surface should be equal to unity is added into the process of computation of the ultimate bearing capacity. Figure 12 shows a homogeneous soil footing without self-weight under vertical loading. The analytical solution of limit load can be obtained by the Prandtl method as expressed in (5.1).

Table 5: Factors of safety by the LEM, SSRM, and FELEM.

Methods	Slope inclination				
	30°	35°	40°	45°	50°
FELEM	1.350	1.280	1.220	1.155	1.088
SSRM	1.340	1.260	1.210	1.150	1.080
LEM	1.334	1.254	1.181	1.113	1.055

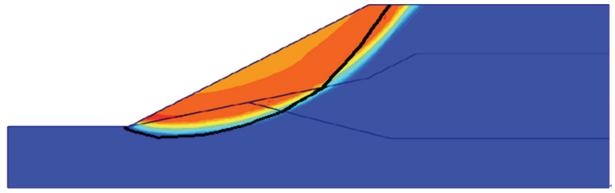

Figure 6: Comparison of critical slip surfaces between the FELEM and SSRM.

Figure 7: Comparison of critical slip surfaces between the FELEM and LEM.

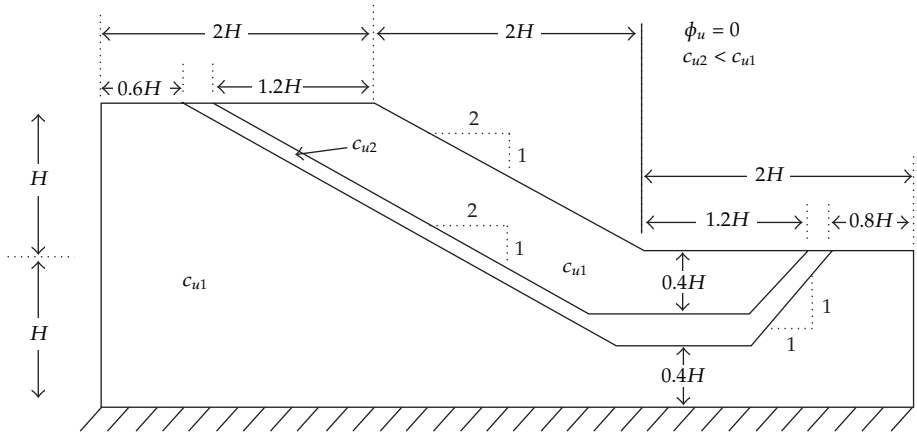

Figure 8: Soil slope with a soft band.

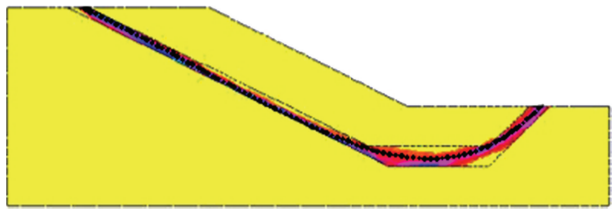

Figure 9: Slip surface comparisons with c_{u2}/c_{u1} equal to 0.5.

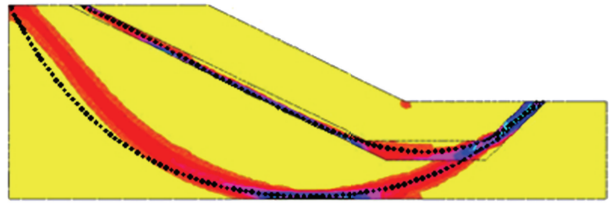

Figure 10: Slip surface comparisons with c_{u2}/c_{u1} equal to 0.6.

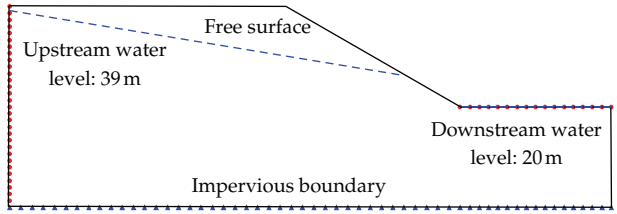

Figure 11: Homogeneous slope under steady-state seepage.

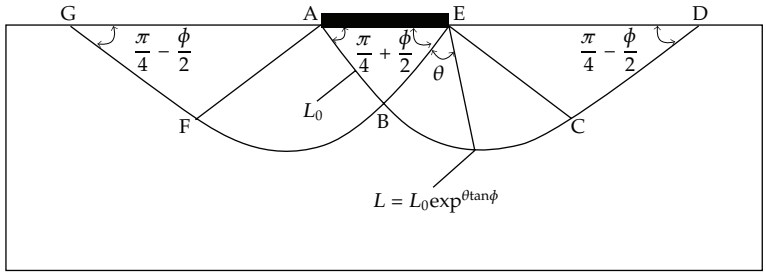

Figure 12: Prandtl solution of homogeneous footing.

The ultimate bearing capacities and locations of critical slip surfaces for the typical cases ($\phi = 25°$) achieved by the FELEM and the theoretical results determined by (5.1) with different friction angles of the slopes are presented in Table 6 and Figure 13

$$P_u = c \cdot \left(\tan^2 \left(\frac{\pi}{4} + \frac{\phi}{2} \right) e^{\pi \tan \phi} - 1 \right) \cdot \cot \phi. \tag{5.1}$$

It can be seen from Table 6 and Figure 13 that the differences concerning the ultimate bearing capacity, the minimum factors of safety, and locations of associated failure surfaces are fairly minor between the FELEM and the analytical method. Thus, it is proven that the FELEM can lead to good estimation on the ultimate bearing capacity and capture the potential failure surface for the soil footing in geotechnical practices.

6. Summary

In the present study, the finite element limit equilibrium method (FELEM) in conjunction with a modified particle swarm optimization algorithm for slope stability evaluation is proposed. A number of remarkable features of this approach are highlighted. It is clearly

Table 6: The results of ultimate bearing capacity (kPa).

Methods		$\phi/(^\circ)$				
		5	10	15	20	25
FELEM	P_u	66.3	85.3	111.8	149.6	204.5
	F_s	1.006	1.010	1.022	1.028	1.038
LEM	P_u	64.9	83.5	109.8	148.5	207.2
	F_s	1.0	1.0	1.0	1.0	1.0

Figure 13: Comparisons of failure surfaces of the FELEM and LEM for Example 5.5.

shown that (i) the definition of factor in the FELEM is suitable for noncircular slip surfaces; (ii) concerning the physical meaning, the factor of safety in the FELEM is the average value of the shear strength reduction coefficient along the sliding surface; (iii) it is still built on the basis of strength reserving theory as that in the LEM and SSRM; (iv) the FELEM in conjunction with the modified particle swarm optimization algorithm can be applied to the determination of non-circular failure surfaces accurately and efficiently; (v) satisfactory agreement on the minimum factors of safety and locations of associated critical surfaces between the LEM, SSRM, and FELEM can be achieved. Consequently, it is proven that the FELEM coupled with the modified particle swarm algorithm can be performed in general geotechnical engineering practice as a beneficial reinforcement for the LEM and SSRM.

Acknowledgments

The financial support by the Foundation of the State Key Laboratory of Coastal and Offshore Engineering (LP1016), the National Nature Science Foundation of China (51009021), and Special Scientific Research Foundation of China Institute of Water Resources and Hydropower Research (Yanji1211) and experimental data and technological supports from Professor Shao Longtan and Dr. Zhao Jie are gratefully acknowledged.

References

[1] Y. M. Cheng, "Location of critical failure surface and some further studies on slope stability analysis," *Computers and Geotechnics*, vol. 30, no. 3, pp. 255–267, 2003.

[2] Z. Teng, J. He, A. J. Degnan et al., "Critical mechanical conditions around neovessels in carotid atherosclerotic plaque may promote intraplaque hemorrhage," *Atherosclerosis*, vol. 223, no. 2, pp. 321–326, 2012.

[3] S. Chen, Y. Wang, and C. Cattani, "Key issues in modeling of complex 3D structures from video sequences," *Mathematical Problems in Engineering*, vol. 2012, Article ID 856523, 17 pages, 2012.

[4] S. Y. Chen, J. Zhang, Q. Guan, and S. Liu, "Detection and amendment of shape distortions based on moment invariants for active shape models," *IET Image Processing*, vol. 5, no. 3, pp. 273–285, 2011.

[5] F. Kang, J. Li, and Q. Xu, "Damage detection based on improved particle swarm optimization using vibration data," *Applied Soft Computing*, vol. 12, no. 8, pp. 2329–2335, 2012.

[6] F. Kang, J. Li, and Z. Ma, "An artificial bee colony algorithm for locating the critical slip surface inslope stability analysis," *Engineering Optimization*. In press.

[7] O. C. Zienkiewicz, C. Humpheson, and R. W. Lewis, "Associated and non-associated visco-plasticity and plasticity in soil mechanics," *Geotechnique*, vol. 25, no. 4, pp. 671–689, 1975.

[8] D. V. Griffiths and P. A. Lane, "Slope stability analysis by finite elements," *Geotechnique*, vol. 49, no. 3, pp. 387–403, 1999.

[9] Y. M. Cheng, T. Lansivaara, and W. B. Wei, "Two-dimensional slope stability analysis by limit equilibrium and strength reduction methods," *Computers and Geotechnics*, vol. 34, no. 3, pp. 137–150, 2007.

[10] J.-Z. Zou, D. J. Williams, and W.-L. Xiong, "Search for critical slip surfaces based on finite element method," *Canadian Geotechnical Journal*, vol. 32, no. 2, pp. 233–246, 1995.

[11] J. Y. Kim and S. R. Lee, "An improved search strategy for the critical slip surface using finite element stress fields," *Computers and Geotechnics*, vol. 21, no. 4, pp. 295–313, 1997.

[12] H. T. V. Pham and D. G. Fredlund, "The application of dynamic programming to slope stability analysis," *Canadian Geotechnical Journal*, vol. 40, no. 4, pp. 830–847, 2003.

[13] T. Yamagami and Y. Ueta, "Search for critical slip lines in finite element stress fields by dynamic programming," in *Proceedings of the 6th International Conference on Numerical methods in Geomechanics*, pp. 1347–1352, Innsbruck, Austria, 1988.

[14] L. T. Shao, H. X. Tang, and G. C. Han, "Finite element method for slope stability analysis with its applications," *Chinese Journal of Computational Mechanics*, vol. 18, no. 1, pp. 81–87, 2001.

[15] Y. M. Cheng, L. Li, S.-C. Chi, and W. B. Wei, "Particle swarm optimization algorithm for the location of the critical non-circular failure surface in two-dimensional slope stability analysis," *Computers and Geotechnics*, vol. 34, no. 2, pp. 92–103, 2007.

[16] V. R. Greco, "Efficient Monte Carlo technique for locating critical slip surface," *Journal of Geotechnical Engineering*, vol. 122, no. 7, pp. 517–525, 1996.

[17] A. I. H. Malkawi, W. F. Hassan, and S. K. Sarma, "Global search method for locating general slip surface using Monte Carlo techniques," *Journal of Geotechnical and Geoenvironmental Engineering*, vol. 127, no. 8, pp. 688–698, 2001.

[18] S. Chen, Y. Zheng, C. Cattani, and W. Wang, "Modeling of biological intelligence for SCM system optimization," *Computational and Mathematical Methods in Medicine*, vol. 2012, Article ID 769702, 10 pages, 2012.

[19] P. Lu, S. Chen, and Y. Zheng, "Artificial intelligence in civil engineering," *Mathematical Problems in Engineering*, vol. 2013, Article ID 145974, 20 pages, 2013.

[20] Z. Jie, *The research of some application problems in finite element method for slope stability analysis [Ph.D. thesis]*, Dalian University of Technology, Dalian, China, 2006.

[21] D. V. Griffiths, "Computation of bearing capacity factors using finite elements," *Geotechnique*, vol. 32, no. 3, pp. 195–202, 1982.